Journal of Inorganic and General Chemistry
ZAAC
Zeitschrift für anorganische und allgemeine Chemie
www.zaac.wiley-vch.de
RESEARCH ARTICLE
Check for updates
DOI: 10.1002/zaac.202300229

Synthesis of the $(Sn_4Bi_4)^{2-}$ Anion by Mild Oxidation of $(Sn_2Bi_2)^{2-}$

Yannick R. Lohse,[a] Bastian Weinert,[a] Benjamin Peerless,[a] and Stefanie Dehnen*[a]

Dedicated to Prof. Dr. Michael Ruck on the occasion of his 60th birthday.

Reactions involving Zintl ions are typically carried out in N-based solvents such as liquid ammonia ($NH_{3(l)}$), ethane-1,2-diamine (*en*), pyridine (*py*), or acetonitrile (CH_3CN). We are currently investigating the application of other solvents as alternatives. Herein, we present the synthesis of the $(Sn_4Bi_4)^{2-}$ anion, obtained as its $[K(crypt\text{-}222)]^+$ salt (crypt-222 = 4,7,13,16,21,24-hexaoxa-1,10-diazabicyclo[8.8.8]hexacosane), from reactions of the binary, *pseudo*-tetrahedral Zintl anion $(Sn_2Bi_2)^{2-}$ in the presence of phosphines as oxidation agents in *ortho*-difluorobenzene (*o*-DFB). The cluster comprises 38 valence electrons, hence, represents an *arachno*-type architecture according to *Wade-Mingos* rules. Micro-X-ray fluorescence (μ-XFS) spectroscopy rationalized the elemental composition of the anion, and quantum chemical studies served to compare the stability of possible structural isomers of the global minimum structure.

Introduction

The extraction of Zintl phases, intermetallic solids typically of potassium with p-block elements, with polar solvents is a common strategy for making soluble, molecular Zintl anions available for chemical reactions in solution. So far, liquid ammonia ($NH_{3(l)}$), ethane-1,2-diamine (*en*), pyridine (*py*), and acetonitrile (CH_3CN) have been the most commonly used solvents for that purpose, and also for subsequent reactions of the extracted Zintl anions.[1] Due to their large relative permittivity, these solvents not only dissolve the solids, but also stabilize highly charged clusters by solvation. Clusters with high anionic charges per atom, such as the series of Tt_4^{4-} (Tt = tetrel = group 14 element) anions,[2,3] can only be stabilized in $NH_{3(l)}$, which additionally has the added benefit of coordinating to the alkali metal cation. When using *en*, *py*, or CH_3CN as a reaction medium, alkali metals are usually sequestered by crown ethers or cryptands, such as 18-crown-6 (1,4,7,10,13,16-hexaoxacyclo-octadecane) or crypt-222 (4,7,13,16,21,24-hexaoxa-1,10-diazabicyclo[8.8.8]hexacosane). Such solvents, however, can only dissolve and stabilize salts of anions with a relatively low charge per atom in the cluster, e.g., Ge_9^{4-}.[4]

We are currently aiming at exploring other potential solvents for reactions of compounds containing Zintl ions. Using the relative permittivity ε_r of the solvents as a selecting parameter, we identified *ortho*-difluorobenzene (*o*-DFB, ε_r = 13.38 at 301.2 K) as a potentially suitable solvent in Zintl chemistry, which should be performing similarly as *en* (ε_r = 13.82 at 293.2 K) and *py* (ε_r = 13.26 at 293.2 K).[5]

To test the suitability of this new uncommon solvent in the context of Zintl chemistry, the solubility and stability of binary *pseudo*-tetrahedral Zintl anions was investigated. Furthermore, the behavior of such anions in the presence of mild oxidants was additionally investigated. Here, we present the results of reactivity studies of $[K(crypt\text{-}222)]_2(Sn_2Bi_2)\cdot en$ towards benzophenone, triphenylphosphine (PPh_3), (ethane-1,2-diyl)bis(diphenylphosphane) (dppe), and (propane-1,3-diyl)bis(diphenylphosphane) (dppp).

Results and Discussion

$[K(crypt\text{-}222)]_2(Sn_2Bi_2)\cdot en$ was prepared as per the published procedure by extraction of 'KSnBi' with crypt-222 in *en* and dissolved in *o*-DFB. A dark red brown solution forms immediately, and appears to be stable for a few hours, whereupon the precipitation of a black powder, presumably Sn and Bi, occurs and a loss of color of the supernatant solution is observed. Nevertheless, the metastability of the compound did not hinder further reactions in this solvent. When one equivalent of benzophenone was added to the reaction mixture, the color of the reaction solution gained a blue tint, an indication of the formation of the ketyl radical. Typically, benzophenone is an unsuitable reagent in Zintl chemistry as it readily reacts with the *en* solvent. However, after filtration of the reaction solution, layering with toluene and storing at −10 °C, brown, block-like crystals of the previously described $[K(crypt\text{-}222)]_2(Sn_7Bi_2)\cdot en\cdot tol$ formed.[6] Upon changing the oxidant to

[a] Y. R. Lohse, Dr. B. Weinert, Dr. B. Peerless, Prof. Dr. S. Dehnen
Institute of Nanotechnology
Karlsruhe Institute of Technology
Kaiserstraße 12, 76131 Karlsruhe, Germany
E-mail: stefanie.dehnen@kit.edu

Supporting information for this article is available on the WWW under https://doi.org/10.1002/zaac.202300229

phosphines, however, after crystallization, brown, block-like crystals of $[K(crypt\text{-}222)]_2(Sn_4Bi_4)_{0.9}(Sn_7Bi_2)_{0.1}\cdot tol$ (**1**) were isolated instead, a new 8-atom cluster of Sn and Bi. No matter which phosphine, PPh_3, dppe, or dppp, was used, the outcome was the same.

Compound **1** crystallizes in the triclinic crystal system (space group type $P\bar{1}$, $Z=2$). Figure 1 shows the molecular structure of the cluster anion $(Sn_4Bi_4)^{2-}$ in **1** and the packing scheme of the major components in the crystal according to single-crystal X-ray diffraction (XRD).

The cluster anion $(Sn_4Bi_4)^{2-}$ is an *arachno*-type cluster with $n=8$ vertices as according to Wade-Mingos rules.[7,8] It comprises of 38 valence electrons, or $4\cdot5+4\cdot4+2-16=22=2\cdot8+6$ (i.e., $2\cdot n+6$) skeletal electrons. Like all known eight-vertex *arachno*-type clusters, it can be derived from a two-capped square antiprism as its parental *closo*-architecture.

In the cluster in **1**, one of the capping positions and one of the positions of the square antiprism are unoccupied, thus, the unoccupied positions are not neighboring sites. As illustrated in Figure 2, this structure (denoted as **ST1**) is only one of three possible ways of deriving the *arachno*-cluster from the *closo*-type species, and could be called the "meta" variant. A "para" variant is represented by structure **ST2**, obtained by formally removing the two opposite capping vertices, while only the "ortho" variant (structure **ST3**), in which neighboring atoms

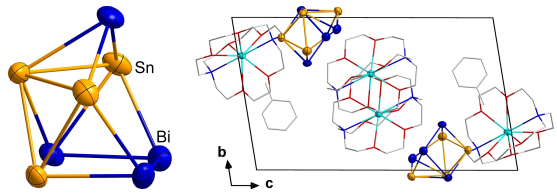

Figure 1. Molecular structure of the $(Sn_4Bi_4)^{2-}$ anion in **1** (left) and view of the extended unit cell (right; K: turquoise, N: blue, O: red, C: grey; minority component not shown). Thermal ellipsoids of Sn, and Bi atoms are shown at 50% probability. More details about the XRD data are provided in the Supporting Information. Selected distances [Å] and angles [°]: Sn–Sn 3.061(4)–3.427(2), Bi–Bi 2.987(1)–3.021(1), Sn–Bi 2.902(2)–3.080(2); Sn–Sn–Sn 58.46(7)–99.08(7), Bi–Sn–Sn 53.25(3)–110.18(8), Sn–Bi–Sn 59.73(8)–107.24(3), Bi–Bi–Bi 91.40(2), Sn–Bi–Bi 57.41(2)–108.19(3), Bi–Sn–Bi 60.33(3)–105.57(4).

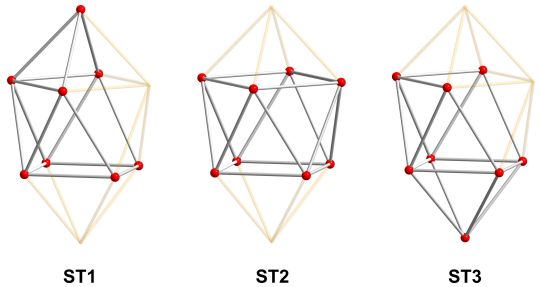

Figure 2. Different variants of eight-vertex *arachno*-type cluster structures, **ST1** (left), **ST2** (center) and **ST3** (right). Additional bonds drawn in semi-transparent mode illustrate the relationship with the parental 10-vertex *closo*-type architecture.

are formally removed, would accord with the construction rules of borane cages.[9]

ST1 has already been realized with the anions $(Sn_4Sb_4)^{2-}$ (Figure 3a) in $[K(crypt\text{-}222)]_2(Sn_4Sb_4)$ (**A**) and $(Sn_5Sb_3)^{3-}$ (Figure 3b) in $[^nBu_4P]_3(Sn_5Sb_3)$ (**B**).[10,11] Compounds comprising clusters with **ST2**-type architectures are also known, but not for the elemental combination of Sn/Bi nor that of Sn/Sb, but only with the respective homoatomic clusters, like the Sn_8^{2-} anion, which is present in compounds $A_4Li_2Sn_8$ (A = Rb, K) obtained from solid-state reactions (Figure 3c).[12] The isostructural Sb_8^{2+} cation was observed in the compounds $Sb_8[GaX_4]_2$ (X = Br, Cl).[13,14] The largest variety of compounds based on tetragonal antiprisms are those comprising the Bi_8^{2+} cation, thus $Bi_8[X]_2$ ($X=AlCl_4$, $GaCl_4$, $InBr_4$),[15–17] $Bi_8A[AlCl_4]_3$ (A = Cs, Rb),[18] $(Bi_8)Bi[InI_4]_9$, and $Bi_8[Ta_2O_2Br_7]_2$.[19,20] Two further, non-deltahedral eight-vertex anions are $(Sn_3Bi_5)^{3-}$ (Figure 3d), which was isolated from solution as its [Rb(crypt-222)]-salt, and $(Sn_4Bi_4)^{4-}$ (Figure 3e), which could be crystallized as a $[Cs([18]crown\text{-}6)]^+$ salt.[21,22] Nevertheless, these two examples are more electron-rich (40 valence electrons or 24, i.e., $2\cdot n+8$, skeletal electrons), and would therefore comply with *hypho*-type cluster units according to *Wade-Mingos* rules; indeed, capping of the square face and the two pentagonal faces would lead these structures back to a parental 11-vertex *closo*-type architecture.

While the structure and electronic situation of the cluster in **1** differs notably from those observed for $(Sn_3Bi_5)^{3-}$ and $(Sn_4Bi_4)^{4-}$,[21,22] it possesses the same structure and total electron count as the Sn/Sb-based Zintl anion in compound **B**.[11] However, the atomic ratios differ, which correlates with different anionic charges of the two related anions. Disregarding the Bi versus Sb atoms, the anions can be transferred into each other by isoelectronic replacement of one Sn^- atom in **B** by a neutral group 15 atom in **1**. The atomic distances in the $(Sn_4Bi_4)^{2-}$ anion correspond to the expected values.[6,21,22]

It should be noted that the $(Sn_4Bi_4)^{2-}$ anion in **1** is the majority component (90%) in a salt that comprises the nine-atom cage $(Sn_7Bi_2)^{2-}$, which was previously reported in another compound,[6] as the minority component (10%). Both anions are located on the same anionic position in the crystal, which we ascribe to the fact that they have very similar sizes (differing by one atom only) and the same charge. The co-crystallization is well reflected in the results of a micro X-ray fluorescence spectroscopy (μ-XFS) analysis, which confirm an elemental composition Sn : Bi of 1.13 : 1

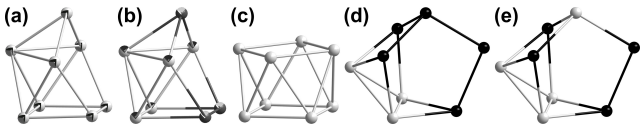

Figure 3. Structures of eight-vertex anions. a) $(Sn_4Sb_4)^{2-}$,[10] b) $(Sn_5Sb_3)^{3-}$,[11] c) Sn_8^{2-} (as a representative also for Sb_8^{2+} and Bi_8^{2+}),[12] d) $(Sn_3Bi_5)^{3-}$,[21] e) $(Sn_4Bi_4)^{4-}$.[22] Bicolor ellipsoids indicate mixed occupation.

Potential isomers and isoelectronic variations of the $(Sn_5Sb_3)^{3-}$ anion were previously studied with detailed quantum chemical calculations using DFT methods.[11] This study indicated the **ST1** isomer to be the preferred one for the Sn/Sb elemental combination in a 5:3 ratio of atoms and a 3− charge. However, the study also indicated that isoelectronic replacement within the $(Sn_{8-x}Sb_x)^{(6-x)-}$ series does not always yield the same structure as the preferred one.

For comparison, we performed DFT calculations on the $(Sn_4Bi_4)^{2-}$ anion in **1** and related *arachno*-type variants. The calculations were done without symmetry restrictions (C_1) of the molecules using the program system TURBOMOLEv7.2,[23] the TPSSH functional,[24] and dhf-TZVP basis sets[25] including corresponding auxiliary bases and effective core potentials.[26,27] The conductor-like screening model (COSMO)[28] was applied for charge compensation. All possible distributions of the four Sn and four Bi atoms over the atomic sites of the three *arachno*-type structures, **ST1**, **ST2**, and **ST3**, were considered for simultaneous optimization of geometric and electronic structures. Notably, structures of the **ST3** type did not converge as such; another variant of that type was observed instead, with slightly varied structural features, denoted as **ST3'**.

The most energetically favorable isomers as well as the least favorable isomer of the three sets of calculations are summarized in Figure 4 along with their relative energies with regard to the lowest energy isomer. The resulting total and relative energies of all isomers with regard to the lowest energy isomer are given in Tables S4–S9.

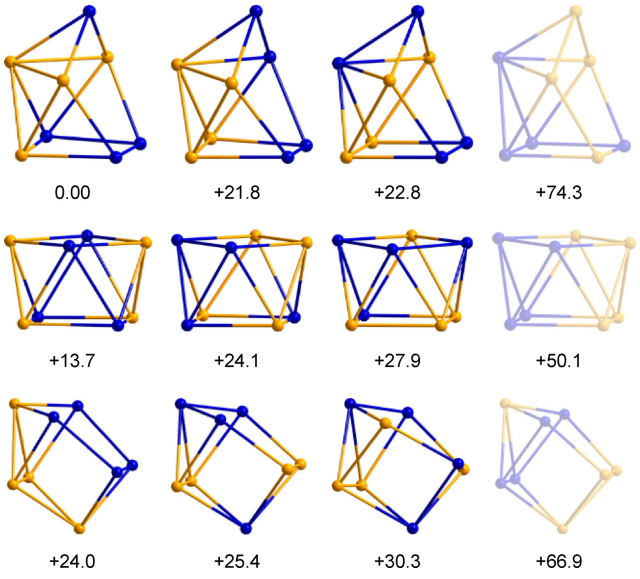

Figure 4. Structures of the three energetically most favorable isomers (from left to right) as well as the least favorable isomer (semi-transparent representation, right) of the computed $(Sn_4Bi_4)^{2-}$ anion in **1** upon geometry optimization of the **ST1** (top), **ST2** (center), and **ST3'** (bottom) types. Relative energies are given in kJ·mol^{-1} with respect to the global minimum structure (**ST1**, top left). Color scheme: Sn (orange), Bi (blue).

The most stable variant of the **ST1** structure type (Figure 4, top left) is the global minimum structure of all $(Sn_4Bi_4)^{2-}$ isomers. Hence, the anion experimentally observed in crystalline compound **1** represents the lowest energy isomer of this composition. With a difference of 21.8 kJ·mol^{-1}, the isomer with the next highest energy of **ST1** is already significantly less favorable than the global minimum structure. This explains why we do not observe a (partial) disorder of Sn and Bi atoms over different atomic sites in this cage, like in other Sn/Bi-based Zintl anions and clusters, but are able to make a clear atom assignment. We asked ourselves what makes this isomer more favorable. Larger numbers of heteroatomic bonds were previously given as an argument for enhanced stability; however, the **ST1** isomer #3 (Figure 4, top row, third from left) has a larger number of heteroatomic bonds (10) than the global minimum structure (8). A more detailed analysis of the situation in the cluster isomers indicate that the correlation of stability with the number of heteroatomic contacts is actually only valid for 3- and 4-connected atoms in **ST1**, yet not so for the 5-connected atoms (see Figure S9).

Also, symmetry does not seem to be the dominant factor for the energetic preferences, as this would favor structure type **ST2** overall (idealized D_{4d} symmetry), and within the **ST1** series, again, isomer #3 (possessing idealized C_s symmetry).

However, the highly symmetric structure type **ST2** is only the second most stable structural variant. In the preferred isomer of the **ST2** type, the atoms are indeed distributed in a way that allows for a maximum of heteroatomic bonds (12 out of 16) besides only 4 homoatomic bonds (Figure 4, center left), which in this case is due to the fact that all atoms are 4-connected and equal in their coordination environment. Nevertheless, this isomer is 13.7 kJ·mol^{-1} higher in energy than the global minimum isomer of **ST1**, which is a notable energetic disadvantage and supports the observation that **ST2** has never been found experimentally for naked heteroatomic eight-atom cages so far.

Unlike for the DFT calculations of isomers of the types **ST1** and **ST2**, none of the geometry optimizations of the 38 isomeric anions according to variant **ST3** converged in the corresponding topology. Although **ST3** also corresponds to an *arachno*-type cluster, it does not seem to offer the opportunity for a local energetic minimum. Instead, 21 anions converged into isomers of the **ST1** type, and 11 yielded structures of type **ST2**. For 6 isomers, the geometry optimization resulted in a slightly distorted variant (**ST3'**, Figure S7), which can be derived from **ST3** by bond breaking in the four-membered "middle deck". In addition, an unsymmetric distribution of Sn and Bi atoms on the cluster sites causes significant distortion of the cage (see Figure S8 for detailed comparison). Again, symmetry is not a major factor for stability though for this structure type, as the loss of the mirror plane when going from isomer #2 to isomer #3 leads to a slight energetic disadvantage only, while the least stable **ST3'**-type isomer (66.9 kJ·mol^{-1} higher in energy than the global minimum structure) possesses C_s symmetry again. As a matter of fact, the number of heteroatomic versus homoatomic bonds does not seem to have a major influence on the order of isomers in

energy for structure type **ST3'**–isomers #1 and #2 are nearly isoenergetic, but exhibit 6 or 10 heteroatomic bonds (out of 14), respectively.

We mention in passing that a change of structure types during geometry optimization also occurs for the other structure types: Three of the isomers from **ST1** converge in **ST3'**, and of the 38 possible isomers, many others converge to different sets of the same isomers, so that ultimately, only 14 independent isomers of the **ST1** structure type were computed (Figure S5). **ST2** is an exception, as here, every conceivable isomer leads to a local minimum structure within the framework of the DFT studies (Figure S6).

The results are in agreement with those reported for the $(Sn_{8-x}Sb_x)^{(6-x)-}$ series: For an equivalent ratio of both elements these studies also predicted the most stable isomer to be of the **ST1** type, followed by **ST2** and finally **ST3'**, but the 4:4 distribution of Sn and Sb atoms was not observed in that study.[11] Instead, it was reported very recently as an intermediate product of the reaction of $[K(crypt\text{-}222)]_2(Sn_2Sb_2)$·*en* with $[U(C_5Me_4H)Cl]$ in *en*.[10]

Conclusions

We presented the treatment of the Zintl salt $[K(crypt\text{-}222)]_2(Sn_2Bi_2)$·*en* with the oxidizing agents benzophenone, PPh_3, dppe, and dppp in *o*-DFB. The reactions did not only prove the suitability of *o*-DFB as a solvent in this context, but also yielded a new compound comprising the previously unknown binary Zintl anion $(Sn_4Bi_4)^{2-}$. As *o*-DFB is largely inert to the reactants used–in striking contrast to the commonly used solvent *en*–the oxidants were both necessary and also proven to be responsible for the oxidations. The *arachno*-type topology of this anion has been reported for other elemental compositions, but a 4:4 ratio of Sn and Bi atoms has no precedence. DFT calculations were used to study the relative stabilities of different isomers–both different distributions of Sn and Bi atoms on the atomic positions of the 8-vertex cage and also different structure types. This way, the structure type observed in compound **1**–although not being the most symmetrical one–was determined to be the most energetically favorable isomer.

Experimental Section

Please see the supporting information for details regarding syntheses and analyses of the title compound.

Acknowledgements

The authors gratefully acknowledge financial support from the Deutsche Forschungsgemeinschaft (DFG, German Research Foundation) through the Collaborative Research Centre "4f for Future" (CRC 1573, project number 471424360), project A3. The work was co-funded by the European Union (ERC, BiCMat, 101054577). Views and opinions expressed are however those of the author(s) only and do not necessarily reflect those of the European Union or the European Research Council. Neither the European Union nor the granting authority can be held responsible for them. The authors gratefully acknowledge the support by the Karlsruhe Nano Micro Facility (KNMFi). Open Access funding enabled and organized by Projekt DEAL.

Conflict of Interest

The authors declare no conflict of interest.

Data Availability Statement

The data that support the findings of this study are available from the corresponding author upon reasonable request.

Keywords: Zintl anions · Tin · Bismuth · Single-crystal X-ray analysis · DFT calculations

[1] R. J. Wilson, N. Lichtenberger, B. Weinert, S. Dehnen, *Chem. Rev.* **2019**, *119*, 8506–8554.
[2] C. B. Benda, T. Henneberger, W. Klein, T. F. Fässler, *Z. Anorg. Allg. Chem.* **2017**, *643*, 146–148.
[3] K. Wiesler, K. Brandl, A. Fleischmann, N. Korber, *Z. Anorg. Allg. Chem.* **2009**, *635*, 508–512.
[4] C. H. E. Belin, J. D. Corbett, A. Cisar, *J. Am. Chem. Soc.* **1977**, *99*, 7163–7169.
[5] D. R. Lide, C. Wohlfarth, *CRC Handbook of Chemistry and Physics*, 89th ed., part 6, Taylor & Francis, CRC Press, Boca Raton **2009**, p.6–148.
[6] a) F. Lips, S. Dehnen, *Angew. Chem. Int. Ed.* **2009**, *48*, 6435–6438;b) F. Lips, S. Dehnen, *Angew. Chem. Int. Ed.* **2011**, *50*, 955–959.
[7] K. Wade, *Adv. Inorg. Chem. Radiochem.* **1976**, *18*, 1–66.
[8] D. M. P. Mingos, *Acc. Chem. Res.* **1984**, *17*, 311–319.
[9] R. W. Rudolph, W. R. Pretzer, *Inorg. Chem.* **1972**, *11*, 1974–1978.
[10] K. Beuthert, B. Weinert, R. J. Wilson, F. Weigend, S. Dehnen, *Inorg. Chem.* **2023**, *62*, 1885–1890.
[11] R. J. Wilson, F. Weigend, S. Dehnen, *Angew. Chem. Int. Ed.* **2020**, *59*, 14251–14255; *Angew. Chem.* **2020**, *132*, 14357–14361.
[12] S. Bobev, S. C. Sevov, *Angew. Chem. Int. Ed.* **2000**, *39*, 4108–4110; *Angew. Chem.* **2000**, *39*, 4108–4110.
[13] A. N. Kuznetsov, B. A. Popovkin, *Z. Anorg. Allg. Chem.* **2002**, *628*, 2179–2179.
[14] A. N. Kuznetsov, B. A. Popovkin, K. Ståhl, M. Lindsjö, L. Kloo, *Eur. J. Inorg. Chem.* **2005**, *2005*, 4907–4913.
[15] J. Beck, C. J. Brendel, L. Bengtsson-Kloo, B. Krebs, M. Mummert, A. Stankowski, S. Ulvenlund, *Chem. Ber.* **1996**, *129*, 1219–1226.
[16] M. Lindsjö, Andreas Fischer, L. Kloo, *Eur. J. Inorg. Chem.* **2005**, 670–675.
[17] A. N. Kuznetsov, B. A. Popovkin, *Z. Anorg. Allg. Chem.* **2002**, *628*, 2179–2179.
[18] M. Knies, M. Ruck, *Z. Naturforsch. B* **2021**, *76*, 585–589.
[19] A. Wosylus, V. Dubenskyy, U. Schwarz, M. Ruck, *Z. Anorg. Allg. Chem.* **2009**, *635*, 1030–1035.
[20] J. Beck, T. Hilbert, *Eur. J. Inorg. Chem.* **2004**, *2004*, 2019–2026.
[21] U. Friedrich, N. Korber, *ChemistryOpen* **2016**, *5*, 306–310.

[22] U. Friedrich, M. Neumeier, C. Koch, N. Korber, *Chem. Commun.* **2012**, *48*, 10544–10546.
[23] TURBOMOLE V7.2 2017, a development of University of Karlsruhe and Forschungszentrum Karlsruhe GmbH, **1989–2007**, TURBOMOLE GmbH, since 2007; available from http://www.turbomole.com.
[24] V. N. Staroverov, G. E. Scuseria, J. Tao, J. P. Perdew, *J. Chem. Phys.* **2003**, *119*, 12129.
[25] F. Weigend, R. Ahlrichs, *Phys. Chem. Chem. Phys.* **2005**, *7*, 3297–3305.
[26] F. Weigend, *Phys. Chem. Chem. Phys.* **2006**, *8*, 1057.
[27] B. Metz, H. Stoll, M. Dolg, *J. Chem. Phys.* **2000**, *13*, 2563.
[28] A. Schäfer, A. Klamt, D. Sattel, J. C. W. Lohrenz, F. Eckert, *Phys. Chem. Chem. Phys.* **2000**, *2*, 2187–2193.

Manuscript received: November 19, 2023
Revised manuscript received: December 15, 2023
Accepted manuscript online: December 16, 2023

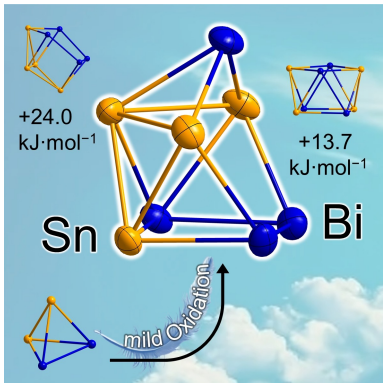

*Y. R. Lohse, Dr. B. Weinert, Dr. B. Peerless, Prof. Dr. S. Dehnen**